Desalination and Water Treatment
www.deswater.com

doi: 10.1080/19443994.2015.1060535

57 (2016) 13701–13710
June

Taylor & Francis
Taylor & Francis Group

Fabrication and characterization of polyethyleneimine immobilized on chloropropyl- and silica-coated magnetic nanoparticles for Pb^{2+} removal from aqueous solution

Laijin Zhong[a], Qi Zhang[a], Menglan Sun[a], Yaling Zhang[a], Hongmei Jiang[a,*], Hongzhen Lian[b,*]

[a]*College of Science, Nanjing Agricultural University, 1 Weigang, Nanjing 210095, China, Tel. +86 15298394576; email: 2013811018@njau.edu.cn (L. Zhong), Tel. +86 05187601; email: 23212111@njau.edu.cn (Q. Zhang), Tel. +86 15651951398; email: 2014811014@njau.edu.cn (M. Sun), Tel. +86 15851800281; email: 609076396@qq.com (Y. Zhang), Tel. +86 25 84396697; Fax: +86 25 84395255; email: jianghongmei@njau.edu.cn (H. Jiang)*
[b]*State Key Laboratory of Analytical Chemistry for Life Science, School of Chemistry & Chemical Engineering and Center of Materials Analysis, Nanjing University, 22 Hankou Road, Nanjing 210093, China, Tel. +86 25 83685941; email: hzlian@nju.edu.cn*

Received 20 November 2014; Accepted 3 June 2015

ABSTRACT

A new surface polymeric functionalized magnetic adsorbent was synthesized through the grafting polyethyleneimine onto chloropropyl- and silica-coated magnetic nanoparticles and characterized by transmission electron microscopy, X-ray diffraction, IR, elemental analysis, and thermo gravimetric analysis. The relationship between grafting reaction conditions, such as solvent, reaction time, reaction temperature, and the polyethyleneimine amount added, and grafting percentage was investigated systematically. Under the optimized conditions, the magnetic adsorbent was fabricated and used for the removal of Pb^{2+} from the solutions for the first time. Batch experiments were carried out to examine the influence of different sorption parameters, for example, solution pH, initial concentration of Pb^{2+}, contact time, and adsorbent dosage. The equilibrium sorption data fitted Langmuir adsorption isotherm well and the adsorbent–adsorbate kinetics followed pseudo-second-order model with a maximum adsorption capacity of 131 mg g^{-1}, which revealed that the prepared polymeric magnetic adsorbent was attractive and effective material with high uptake capacity.

Keywords: Magnetic adsorbent; Surface polymeric functionalization; Adsorption; Pb^{2+}

1. Introduction

Nowadays, the spread of a wide range of metal ions contaminants in surface water and ground water has become a critical issue worldwide. Pb^{2+} is one of such kind of contaminants and has been extensively used in metal processing, electroplating, and electronics leading to large releasing into aquatic environment [1]. Therefore, increasing demands for clean and safe water make it greatly important to develop reliable methods for the removal of Pb^{2+} from environmental waters.

Considerable efforts have been made to establish effective treatment techniques for removing heavy

---

*Corresponding authors.

metal ions from water, and adsorption is regarded as the most attractive method in practical application owing to its simple operation and superior efficiency [2]. In adsorption processes, the choice of an appropriate adsorbent is the key factor to achieve high adsorption capacity, good selectivity, and short analytical time. Recent researches focused on adsorbents such as mineral residues (clinoptilolite and bentonite [3] and clays [4]), biological materials (marine brown algae [5], green alga [6] and bacteria [7]), agricultural and forest wastes [8], and inorganic materials [9] for the removal of heavy metals. As a kind of inorganic absorbent, magnetic nanoparticles (MNPs) exhibit many interesting and remarkable merits including extremely small size, high surface-area-to-volume ratio, facile surface modifiability, and excellent magnetic property and have achieved extensive attention for metal ions removal and environmental applications [10,11]. However, it should be pointed out that naked MNPs are prone to aggregate, not selective and suitable for the samples with complex matrix, and get easily oxidized when exposed to air leading to the loss of magnetic property.

Hence, the development of a proper surface modification is required to protect and keep the stability of MNPs and improve their selectivity. Based on the literatures reported, there are two kinds of primary surface modification methods: physical coating and chemical grafting. With regard to physical coating procedure, coating material and MNPs are mixed together and agitated for a period of time, so it can be also named as co-condensation method [12]. Although this kind modification procedure is simple and convenient, it suffers from lower metal adsorption capacity because of limited loading of functional groups. As for chemical grafting method, MNPs and modified reagent can be integrated firmly through chemical bonding, and the percentage of grafting on MNPs can be tuned by controlling the conditions of the grafting reaction leading to different adsorption capacity. During chemical grafting, MNPs are always firstly coated with silica through hydrolytic and condensation reaction of silane coupling agent as the chemical activity of silicon hydroxyl is greatly higher than that of hydroxyl on the surface of MNPs [13]. Then, large amounts of silicon hydroxyl are introduced into MNPs and a layer of latticed structure of silicon hydroxyl is formed and covered on the surface of MNPs, which can screen the magnetic dipolar attraction between MNPs, improve the dispersion of MNPs in liquid media, and protect magnetic core from leaching under an acidic condition. In particular, the terminal silicon hydroxyls surrounding the surface of MNPs offer ease of functionalization of MNPs. The further grafting materials include different functional groups, for example, amino [14–18], thiol [19–21], and carboxylic [22], which show strong affinity for metal ions enabling specific metal complexation. Up to now, most of researches as mentioned above reported some nonpolymeric organic grafting molecules with less functional groups bringing about lower adsorption capacity.

For enhancing the adsorption capacity of modified MNPs, the modification of MNPs with polymeric reagents not only increases active sites but also makes use of large pores supplied by polymers and has aroused comparative attention for the removal of metal ions. According to the formation processes of polymer MNPs, they can be classified as three groups. The first one is based on direct precipitation of iron salts acted as precursor of MNPs inside the pores of a cross-linked polymer system [23]. During second approach, MNPs are prepared first and then dispersed into different natural polymers for example cellulose [24], gum arabic [25], chitosan [26], and alginate [27–29], which is similar with physical coating. The last method employs MNPs and monomers of polymers as the initial materials, and the mixtures are subsequently polymerized under certain conditions [30]. The limitation with using these *in situ* synthesis routes is that MNPs usually exhibit high tendency to form larger aggregates during blending, which greatly decreases the advantages of their small dimensions.

In this study, we designed a novel protocol for introducing polymers into silica-coated MNPs (Si-MNPs) and named it surface polymeric functionalization. Polyethyleneimine (PEI), a water-soluble chelating polymer containing large amount of amino functional groups [31], was grafted onto the surface of Si-MNPs through nucleophilic substitution between amino and chloropropyl group of silane, which leaded to the formation of a layer of polymer. However, to the best of our knowledge, no attempt has been made to remove aqueous Pb^{2+} using such surface polymeric immobilized Si-MNPs. The effects of different grafting experimental conditions such as solvent, reaction time, reaction temperature, and PEI amount added on adsorption capacity were examined in detail. The newly prepared PEI immobilized on chloropropyl and silica-coated MNPs (PEI-Cl and Si-MNPs) were characterized by elemental analysis (EA), transmission electron microscopy (TEM), X-ray diffraction (XRD), Fourier transform infrared (FT-IR) spectroscopy, and thermo gravimetric analysis (TGA). Some parameters influencing the removal of Pb^{2+} such as solution pH, contact time, adsorbent dose, and initial concentration were investigated. The Langmuir adsorption isotherm and the adsorption–desorption kinetics were both proposed for the present sorption research.

2. Experimental

2.1. Apparatus and instrumentation

PEI-Cl and Si-MNPs were characterized by TENSOR27FT-IR (Bruker, Germany) in the region of 400–4,000 cm^{-1}. The elemental composition on the surface of PEI-Cl and Si-MNPs was measured by Vario EL III Elementar (GmbH, Germany). The size and morphology of PEI-Cl and Si-MNPs were analyzed by JEM-200CX transmission electron microscope (JEOL, Tokyo, Japan). The crystal structure of PEI-Cl and Si-MNPs was examined on ARL X'TRA diffractometer with Cu Kα radiation (ARL, Lausanne, Switzerland). A Hitachi Z-2000 flame atomic absorption spectrometer (FAAS) (Hitachi, Japan) was applied to determine lead concentrations.

The pH of the solution was measured by a Mettler-Toledo FE20 pH meter (Mettler-Toledo, Shanghai, China) supplied with a combined electrode. A KQ3200DE ultrasonic bath (Kunshan Shumei Ultrasonic Instrument, Suzhou, China) was applied to speed up the adsorption process. An Nd–Fe–B magnet (8.0 mm × 6.0 mm × 1.6 mm) was used for magnetic separation.

2.2. Standard solution and reagents

The stock standard solution for Pb (1,000 mg L^{-1}) was bought from China National Measuring Science Research Institute (Beijing, China). Standard solutions were prepared by appropriate dilution of the stock solution daily. All reagents used in the experiments were of analytical grade and purchased from Aladdin's reagent network (Aladdin, Shanghai, China).

2.3. Preparation of PEI-Cl and Si-MNPs

2.3.1. MNPs and Si-MNPs

The preparation of MNPs and Si-MNPs was the same as our previous work [32]. Briefly, MNPs were prepared by coprecipitation of $FeCl_3$ and $FeCl_2$, and Si-MNPs were obtained by wrapping up a layer of silica through hydrolytic and condensation reaction of silylating reagent tetraethoxysilane (TEOS).

2.3.2. Chloropropyl-coated- Si-MNPs (Cl and Si-MNPs)

In order to graft PEI on the surface of Si-MNPs successfully, γ-chloropropyltrimethoxysilane was selected as a coupling agent to chemically link Si-MNPs with polyethyleneimine. Chloropropyl must be introduced and surrounded on the surface of Si-MNPs by hydrolytic and condensation reaction of γ-chloropropyltrimethoxysilane firstly, which resulted in the formation of chloropropyl-coated-Si-MNPs (Cl and Si-MNPs). That is, 5 g Si-MNPs were added in a mixture of 50 mL dimethylbenzene and 4.9 mL water in a three-necked flask and ultrasonically dispersed for 20 min. Then, 25 mL γ-chloropropyltrimethoxysilane was added in the flask and the mixture was refluxed at 85℃ with continuous stirring for 6 h. After cooled to room temperature, Cl and Si-MNPs were magnetically separated and washed sequentially with acetone and deionized water three times, respectively, and then dried under vacuum at 70℃.

2.3.3. PEI-Cl and Si-MNPs

PEI-Cl and Si-MNPs were obtained by surface polymeric functionalization using nucleophilic substitution between amino group of PEI and chloropropyl group of Cl and Si-MNPs. A certain amount of PEI (50%, w/w) was added in a three-necked flask containing 20 mL solvent, and then, the mixture was homogenized by ultrasonic vibration in water bath. A total of 0.2 g Cl and Si-MNPs and a certain amount sodium hydroxide were added and the mixture was refluxed at desired temperature with continuous stirring for an appropriate time. In order to evaluate the influence of grafting reaction parameters on adsorption capacity of PEI-Cl and Si-MNPs, different solvents including ethanol, isobutyl alcohol, dimethylsulfoxide (DMSO), and N,N-dimethylformamide (DMF), reaction times ranging from 1 to 11 h, reaction temperature in the range of 60–100℃, and varying amount of PEI from 0.04 to 2 g were employed and systematically investigated in this work. Fig. 1 shows the synthesis procedure for PEI-Cl and Si-MNPs.

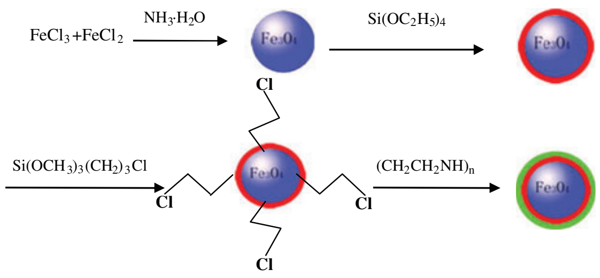

Fig. 1. Procedure for the preparation of PEI-Cl and Si-MNPs.

2.4. Adsorption experiments

All the adsorption studies were conducted in batch modes. Briefly, a certain PEI-Si-MNPs were dispersed into 10 mL of sample solution with the desired pH and the chosen initial concentration of Pb^{2+}. Then, the mixture was blended together and immersed into an ultrasonic bath operated at 40 kHz of ultrasound frequency and 100 W of power to accelerate adsorption progress for a required time. After this, the adsorbent was removed via an external magnetic field and the supernatant was collected for Pb^{2+} determination by AAS.

The effect of initial pH on the recovery of Pb^{2+} ion was evaluated at a pH ranges from 2 to 7. The adsorption behavior was also examined as function of metal ion concentration (5–250 mg L^{-1}), contact time (5–100 min), and adsorbent dosage (5–80 mg). All experiments were run in duplicate and the average values were reported here. The removal percentage ($R\%$) and adsorption capacity (Q, mg g^{-1}) of Pb^{2+} were calculated using Eqs. (1) and (2), relatively:

$$R\% = \frac{(C_o - C_e)}{C_o} \times 100\% \tag{1}$$

$$Q = \frac{(C_o - C_e)V}{M} \tag{2}$$

where C_o and C_e are concentration of Pb^{2+} (mg L^{-1}) in the solutions before and after adsorption, respectively; V is the volume of metal ion solution (L); and W is the weight of the adsorbent (g).

2.5. Desorption and regeneration experiments

A total of 10 mg PEI-Si-MNPs were dispersed into 10 mL 10 mg L^{-1} Pb^{2+} solution and then the mixture was ultrasonicated 30 min to speed up the progress of adsorption. After this, the mixture was magnetically separated and then 10 mL of 0.1 μmol L^{-1} EDTA was added into the beaker as desorption agent and the new mixture was ultrasonicated again for 15 min. Finally, the adsorbent was removed via an external magnetic field and the desorption solution was collected for the determination of Pb by FAAS. After an adsorption–desorption cycle, the adsorbent was washed with deionized water for three times and then directly used for the next cycle. Five sequential cycles of adsorption–desorption were carried out. The desorption percentage ($D\%$) of Pb^{2+} was calculated using following equations:

$$D = \frac{C_d}{C_o} \times 100\% \tag{3}$$

where C_o and C_d are concentration of Pb^{2+} (mg L^{-1}) in the initial solutions and in the desorption solutions, respectively.

3. Results and discussion

3.1. Optimization of PEI-Cl and Si-MNPs synthesis condition

For successful grafting PEI on the surface of Cl and Si-MNPs and improving the thickness of polymer layer as far as possible, the effect of grafting reaction conditions such as solvent, reaction time, reaction temperature, and the PEI dosage on grafting percentage was investigated systematically. To a chelated adsorbent, if all the adsorption experimental condition is constant, adsorption capacity can reflect the amount of functional groups grafted. In this work, it represents the amount of amine on the surface of modified MNPs and thus stands for grafting percent. Moreover, the final objective of this study was the application of newly prepared modified MNPs for the removal of Pb^{2+}; therefore, the effect of different synthetic conditions on the adsorption capacity to Pb^{2+} was studied.

3.1.1. Effect of solvent

The grafting reaction of PEI on the surface of Cl and Si-MNPs is a bimolecular nucleophilic substitution and solvent is a very important parameter. As we all know that polar aprotic solvent or weak polar protic solvent is beneficial to bimolecular nucleophilic substitution, hence, two polar aprotic solvents, DMSO and DMF, and two weak polar protic solvents, ethanol and isobutyl alcohol, were adopted in this work, respectively. As could be seen from Fig. 2(A) that the adsorption capacities using DMSO and isobutyl alcohol as solvents were higher than those using ethanol and DMF. Considering the adsorption capacity of the adsorbent, DMSO was selected as the solvent in the following experiments.

3.1.2. Effect of reaction time

To obtain PEI-Cl and Si-MNPs with high uptake capacity, the effect of reaction time on the adsorption capacity was evaluated as in Fig. 2(B). There was an increasing trend of adsorption capacity with increasing time from 2 to 5 h and then nearly kept unchanged, which illustrated that the grafting reaction was accomplished completely after 5 h. So, 6 h was chosen as reaction time.

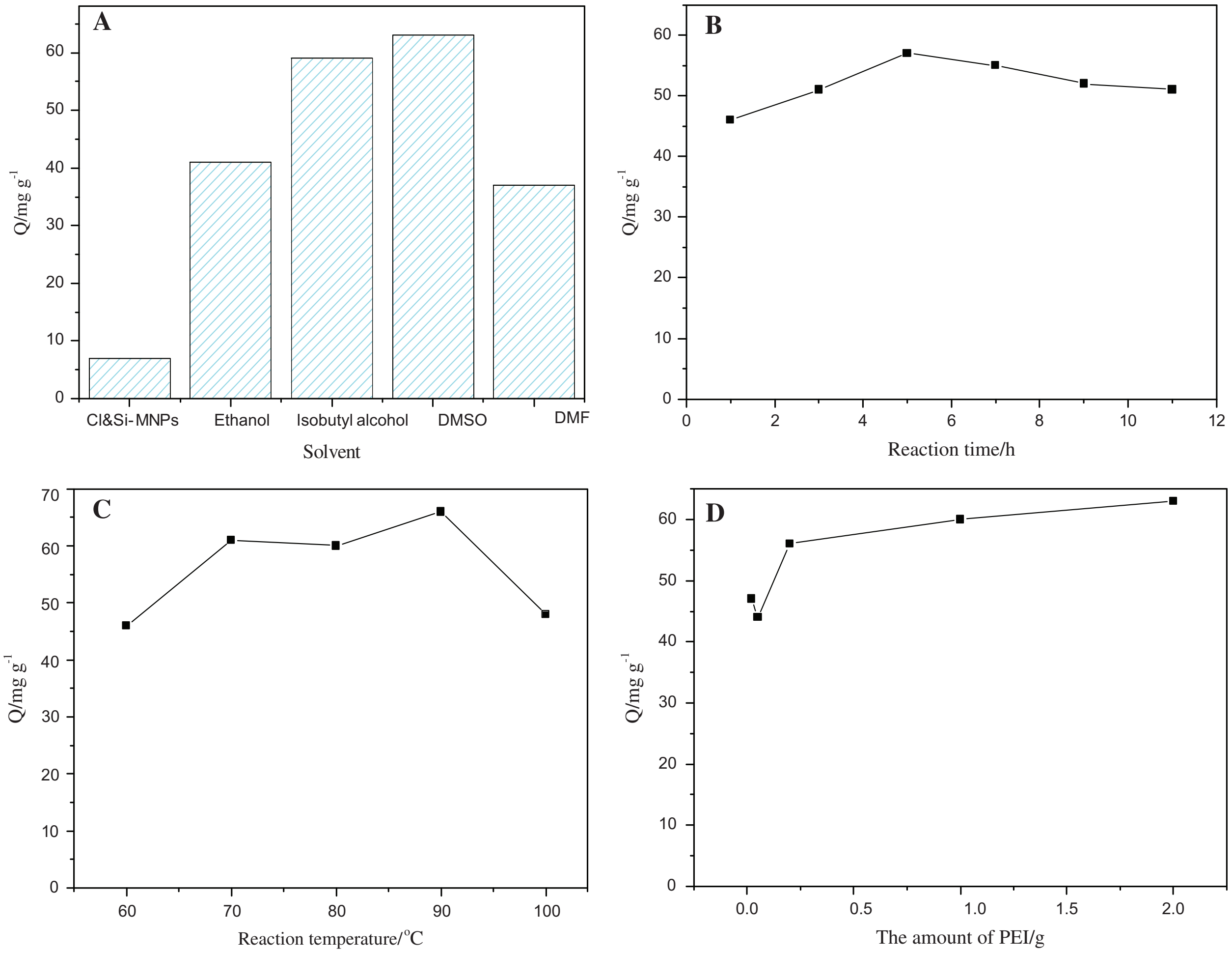

Fig. 2. Effect of grafting reaction conditions including solvent (A), reaction time (B), reaction temperature (C), and the PEI amount added (D) on the adsorption capacity of Pb^{2+}.

3.1.3. Effect of reaction temperature

The effect of reaction temperature on the adsorption capacity was examined and the result was depicted in Fig. 2(C). The reaction temperature was varying from 60 to 100℃. It could be observed that adsorption capacity was improved with the increase of temperature from 60 to 70℃. After that the adsorption capacity remained unchanged until 90℃. When temperature was risen to 100℃, however, the adsorption capacity was decreased instead. Thereby, the reaction was performed at 90℃.

3.1.4. Effect of PEI dosage

In order to learn the relationship between grafting percent or adsorption capacity and the amount of PEI added, the effect of PEI amount varying from 0.04 to 2 g on the adsorption capacity was studied when the amount of Cl and Si-MNPs was fixed at 0.2 g. Fig. 2(D) indicates that the adsorption capacity increased rapidly with the increasing of PEI amount in the range from 0.05 to 0.2 g and then increased very slowly after PEI amount was up to 0.2 g, which demonstrated the complete grafting reaction was reached. Finally, 1.0 g PEI was selected in the following study.

3.2. Characterization of PEI-Cl and Si-MNPs

3.2.1. TEM images

The morphology and structural feature of PEI-Cl and Si-MNPs was observed using TEM. The TEM images shown in Fig. 3 disclosed that the composite magnetic particles were almost uniform and monodisperse and most of them were approximately spherical in shape. The average particle sizes of PEI-Cl and

Si-MNPs were about 15–20 nm and slightly bigger than that of naked MNPs reported in our previous work (Jiang et al. [32]), which implied that a wrapping layer of composite was really introduced on the surface of naked MNPs.

3.2.2. XRD pattern

The crystalline structure of PEI-Cl and Si-MNPs was determined by XRD. The XRD patterns illustrated in Fig. 4 indicated that the composite MNPs were of monophasic and spinel structure. The six characteristic peaks occurred at 2θ region of 20°–70° were marked by their corresponding indices (2 2 0), (3 1 1), (4 0 0), (4 2 2), (5 1 1), and (4 4 0), respectively, which matched well with the standard XRD data cards of Fe_3O_4 crystal (JCPDS No. 19-06290) and reminded that the crystalline structure of synthesized product was not affected by the modification of MNPs. The sharpness of XRD reflections clearly suggested that the composite MNPs were highly crystalline.

3.2.3. FT-IR spectrum

The coating of chloropropyl and Si on MNPs and the functionalization of PEI on Cl and Si-MNPs were confirmed by FT-IR spectra. The spectra for MNPs, Cl and Si-MNPs and PEI-Cl and Si-MNPs were all exhibited in Fig. 5. For all three MNPs, the characteristic peak strongly presented at 582 cm^{-1} was attributed to the Fe–O vibration. The absorption bands at 1,071 cm^{-1} observed on Cl and Si-MNPs and PEI-Cl and Si-MNPs could be ascribed to Si–O stretching vibration, reflecting the formation of a layer of silica on the surface of MNPs. In addition, the absorption peaks at 2,930 cm^{-1} in the spectra of Cl and Si-MNPss and PEI-Cl and Si-MNPs were assigned to $-CH_2-$ group from chloropropyl and PEI. Furthermore, the peaks at 1,653 and 1,446 cm^{-1} in the spectra of PEI-Cl and Si-MNPs were related to N–H bending vibrations, which illustrated that PEI was successfully grafted onto the Cl and Si-MNPs.

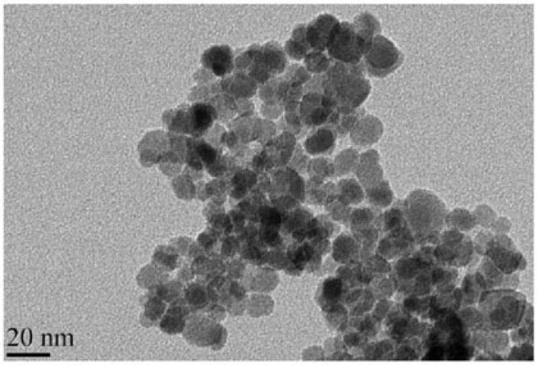

Fig. 3. TEM image of PEI-Cl and Si-MNPs.

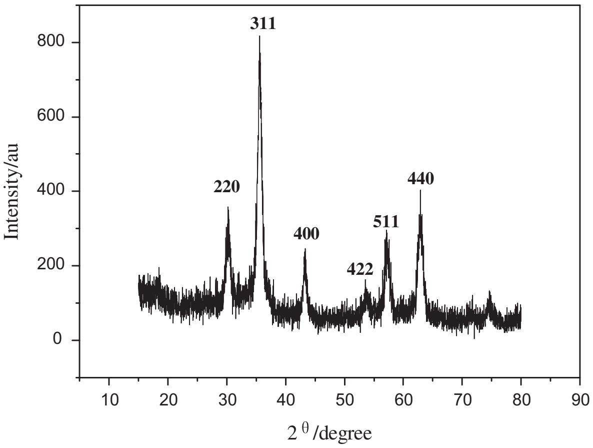

Fig. 4. XRD pattern of PEI-Cl and Si-MNPs.

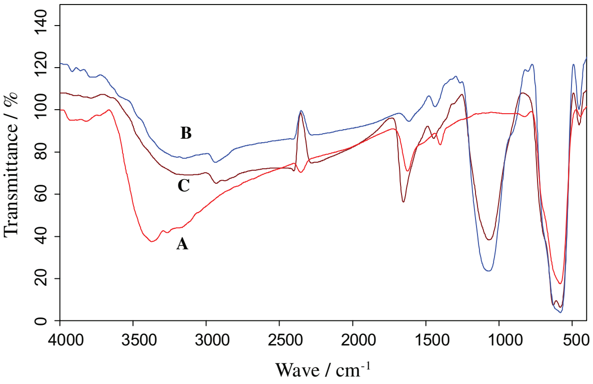

Fig. 5. IR spectra of MNPs (A), Cl and Si-MNPs (B), and PEI-Cl and Si-MNPs (C).

3.2.4. Element analysis

For the determination of major components of the layer organic material wrapped up on the surface of MNPs, the EA was carried out. The contents (wt.%) of carbon, hydrogen, and nitrogen in PEI-Cl and Si-MNPs were 10.63, 1.40 and 0.88%, respectively, which verified further that PEI has been successfully grafted on the surface of Cl and Si-MNPs.

3.3. Adsorption studies

3.3.1. Effect of pH

The pH is one of the most important parameters during adsorption progress because it dominates not only the existing form and solubility of metals but also the degree of protonation of active functional groups possessing acid–base properties on the surface of adsorbent. The relationship between solution pH and adsorption capacity of Pb^{2+} on naked MNPs, Cl and Si-MNPs, and PEI-Cl and Si-MNPs was studied by varying pH in the range of 2–6. It could be observed in Fig. 6(A) that the adsorption capacity of Pb^{2+} on three kinds of materials was all improved with the increasing of pH during the whole pH range. Compared with naked MNPs and Cl and Si-MNPs, the adsorption capacity of Pb^{2+} on PEI-Cl and Si-MNPs increased more rapidly and could be high up to 90 mg g^{-1}. After pH was higher than 6, the further pH effect was not examined due to the easy formation of hydrate precipitation. In other words, the maximum adsorption capacity was achieved at pH 6, which may be resulted from the protonation of amino groups on the surface of PEI-Cl and Si-MNPs and the formation of chelation between N atoms and Pb^{2+}. Based on previous work [33], at low pH value, amino groups were highly protonated, which could be bonded with cations through electrostatic interaction. Under this condition, large amounts of H^+ might compete with Pb^{2+} for the binding sites, leading to the decrease binding with Pb^{2+} and lower capacity. With the increase of solution pH, the protonated degree of the adsorbent declined, the competition from H^+ became weaker, and the chelating ability of N atoms of amino groups toward Pb^{2+} was strengthened and thus the adsorption of Pb was increased, which agreed well with the conclusion in Ref. [34]. At pH 6, the protonation of amino was reduced enough to allow the formation of the metal complexes and the maximal adsorption capacity would be achieved, which was consistent with the apparent pK_a's of PEI between 7 and 9 [35]. So, pH 6 was chosen in the following study.

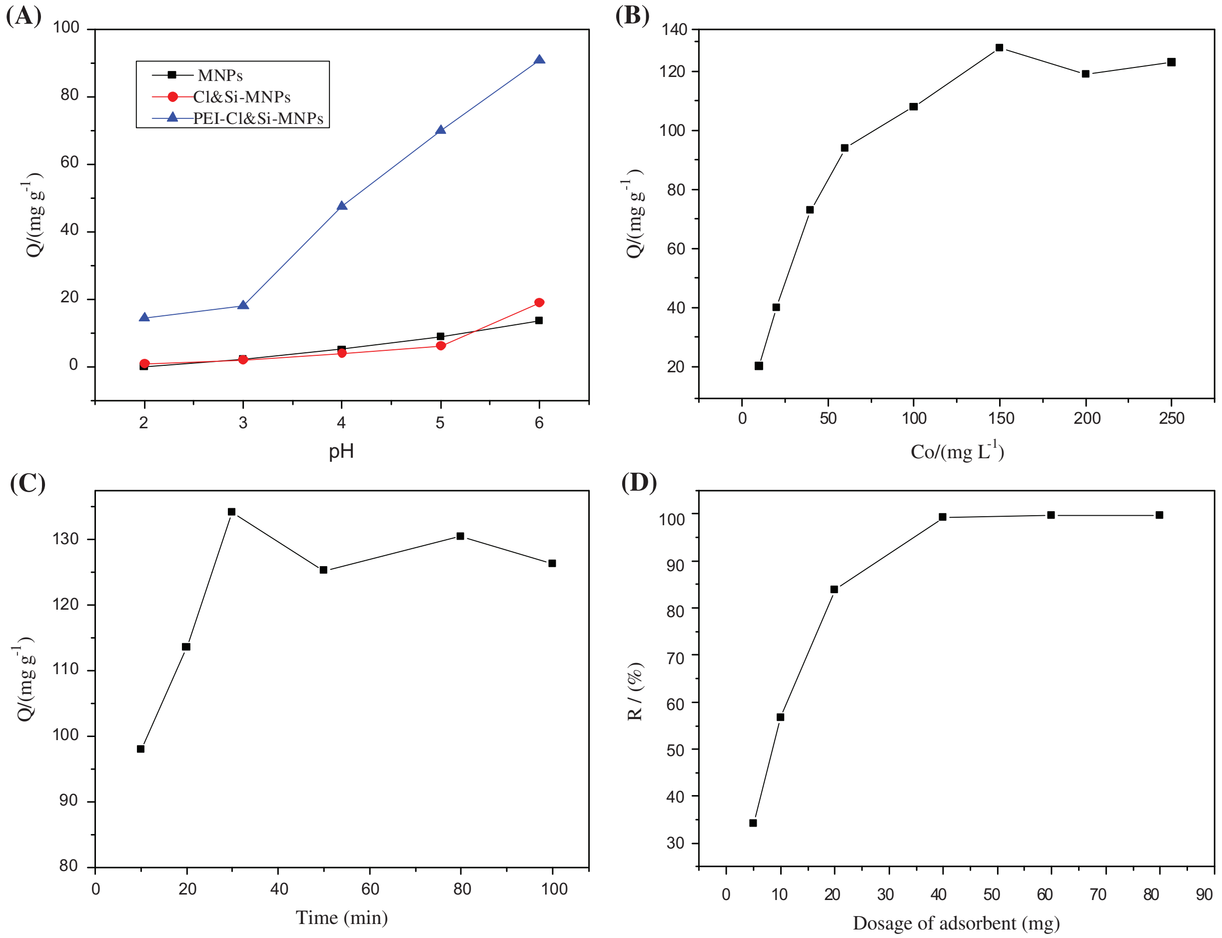

Fig. 6. Effects of pH (A), initial Pb^{2+} concentration (B), and contact time (C) on the adsorption capacity of Pb; and the effect of dosage of adsorbents (D) on the removal percentage of Pb^{2+}.

3.3.2. Effect of initial metal concentration

The initial concentration of Pb^{2+} in solution has a significant influence on the adsorption capacity of Pb^{2+}. The experiments about different Pb^{2+} concentrations were conducted in the range from 10 to 300 mg L^{-1} (Fig. 6(B)). As appeared, uptake capacity was improved rapidly with the increase of initial Pb^{2+} concentration and then attained a saturation value at 150 mg L^{-1} with a maximum equilibrium uptake for Pb^{2+} of about 130 mg g^{-1}. After initial concentration of Pb^{2+} was higher than 150 mg L^{-1}, there was no significant change in adsorption capacity with the initial metal ion concentration. The steep and rapid adsorption during lower initial concentration was attributed to sufficient and available active sites provided by adsorbent and large of Pb^{2+}, which leaded to the interaction between them easily. With the increasing concentration, active sites on the outer surface became exhausted and Pb^{2+} in the solution could only be reacted with inner active sites through longer diffusion, which resulted in a slow adsorption progress and saturated uptake. These results revealed that concentration was the driving force for the metal ions to occupy available adsorption sites and overcome the mass transfer resistance [36]. Furthermore, the data achieved were further applied to explore the isotherm study of the adsorption process.

3.3.3. Effect of contact time

The rates of metal ion adsorption are related to the efficiency of the adsorbent and therefore control the residence contact time of adsorbate at the solid–solution interface. The contact time varying from 5 to 100 min was tested and the results were exhibited in Fig. 6(C). It was apparent that the Pb^{2+} uptake was initially quite high during the first 30 min and followed by a much slower step leading gradually to an equilibrium state. This phenomenon could be explained that after equilibrium adsorption was reached, the surface adsorption sites became less and less, the adsorption capacity was controlled by the rate of transport of Pb^{2+} ions from the exterior to the interior sites of the adsorbent particles. In all subsequent experiments, contact time was maintained at 40 min, which was considered sufficient for the removal of Pb^{2+}. And the data obtained were further used to evaluate the kinetic parameters of the adsorption process.

3.3.4. Effect of adsorbent dosage

Adsorbent dosage is the last important parameter because it determines the removal percentage for a given adsorbent. The adsorption study of Pb^{2+} with different quantity of adsorbent from 5 to 80 mg was performed. As shown in Fig. 6(D), for 200 mg L^{-1} Pb^{2+}, the removal percentage of Pb^{2+} increased with increasing adsorbent dose and then kept constant with nearly 100% removal percentage when the dosage was 40 mg, which could be ascribed to the increase in active sites on the adsorbent, thus making easier penetration of the metal ions to the sorption sites.

3.3.5. Isotherm study

Adsorption isotherm was used to describe the interaction between adsorbent and metal ions, evaluate the uptake capacity, and understand the adsorption mechanism. The Langmuir isotherm model was widely applied to fit the experimental data. Langmuir isotherm equation could be expressed in the following form:

$$\frac{C_e}{q_e} = \frac{1}{k_L Q_{max}} + \frac{1}{Q_{max} C_e} \tag{4}$$

where C_e (mg L^{-1}) is the equilibrium concentration in the solution, q_e (mg g^{-1}) is the equilibrium binding capacity, k_L (L mg^{-1}) is the equilibrium constant related to the binding sites affinity, and Q_{max} (mg g^{-1}) is the maximum binding capacity often used to quantify and compare the performance of different sorbents.

The plots of C_e/q_e vs. C_e gave a liner regression and Q_{max} and k_L calculated from the slopes and interceptions of the lines at different temperatures were listed in Table 1. As observed, high correlation coefficients of the Langmuir equation indicated a good agreement between the parameters and confirmed the monolayer adsorption of Pb^{2+} on PEI-Cl and Si-MNPs.

3.3.6. Kinetic study

The study of sorption kinetic could provide valuable insight into the reaction pathways. The well-known pseudo-second-order kinetics model was selected to fit the experimental kinetic adsorption data. The linearized pseudo-second-order kinetic equation was often used as the following form:

$$\frac{t}{q_t} = \frac{1}{k_2 q_e^2} + \frac{t}{q_e} \tag{5}$$

where q_t (mg g^{-1}) is the amount of adsorption at time t (min), k_2 (g(mg min)$^{-1}$) is the rate constant of the

Table 1
Langmuir parameters and pseudo-second-order parameters for the adsorption of Pb^{2+} on PEI-Cl & Si-MNPs

	Langmuir parameters			Pseudo-second-order parameters		
T (℃)	Q_{max} (mg/g)	k_L (L/mg)	R^2	q_e (mg/g)	k_2 (g/(mg min))	R^2
25	124	0.3277	0.99	131	0.0038	0.99
35	114	0.4693	0.99	118	0.0085	0.99
45	106	0.5183	0.99	114	0.0088	0.99

pseudo-second-order kinetic adsorption, and q_e is the equilibrium adsorption capacity. The values of k_2 and q_e could be achieved from the intercept and slope of the plot of the experimental t/q_t vs. t. The kinetic parameters such as q_e, k_2, and R^2 at different temperatures were listed in Table 1. As illustrated in Table 1, the pseudo-second-order model fitted the adsorption kinetics of Pb^{2+} very well, which indicated that the rate-limiting step controlled the adsorption progress.

3.4. Desorption and regeneration study

Desorption and regeneration performance of MNPs is an important factor as it determines the cost of the adsorption system. To evaluate the possibility of regeneration of PEI-Cl and Si-MNPs, adsorption–desorption experiments were carried out. As a kind of strong chelating agent, EDTA was chosen as desorption agents. In order to desorb Pb^{2+} from the material completely, the effect of the concentration of EDTA on desorption percentage was evaluated in the range of 10^{-4}–10^{-1} mol $L^{-1}$and the results illustrated the whole range of concentration of EDTA could all desorb Pb^{2+} quantitatively. Hence, 0.1 μmol L^{-1} EDTA was used in the regeneration study and the results showed that PEI-Cl and Si-MNPs can be reused 5 cycles without remarkable loss of adsorption performance, which indicated that they had good reusability and great potential for practical application.

4. Conclusions

In this study, a novel surface polymeric functionalized magnetic adsorbent was synthesized through the grafting PEI onto Cl and Si-MNPs, which is simple and cost-effective. Moreover, we found that grafting reaction conditions such as solvent, reaction time, reaction temperature, and the PEI dosage had a remarkable effect on the adsorption performance of Pb^{2+} on PEI-Cl and Si-MNPs. Compared with naked MNPs and Cl and Si-MNPs, the adsorption capacity of Pb^{2+} on PEI-Cl and Si-MNPs was much higher and could be high up to 131 mg g^{-1}. The high adsorption capacity was due to plenty of amino groups and the high adsorption affinity of PEI-Cl and Si-MNPs. And the absorbed Pb^{2+} could be desorbed by 0.1 μmol L^{-1} EDTA, and PEI-Cl and Si-MNPs could be reused 5 cycles without notable loss of adsorption performance, which indicated that they had good reusability and great potential for practical application.

Acknowledgments

This work was supported by Jiangsu Province Science Foundation for Youths (BK20140677), Jiangsu Overseas Research & Training Program for University Prominent Young & Middle-aged Teachers and Presidents, Fundamental Research Funds for the Central Universities (KYZ201220), the National Basic Research Program of China (973 program, 2011CB911003, 2009CB421601), National Natural Science Foundation of China (21275069, 21121091), and Analysis & Test Fund of Nanjing University.

References

[1] Z. Reddad, C. Gérente, Y. Andrès, J. Thibault, P. Le Cloirec, Cadmium and lead adsorption by a natural polysaccharide in MF membrane reactor: Experimental analysis and modelling, Water Res. 37 (2003) 3983–3991.
[2] W.S. Wan Ngah, M.A.K.M. Hanafiah, Removal of heavy metal ions from wastewater by chemically modified plant wastes as adsorbents: A review, Bioresour. Technol. 99 (2008) 3935–3948.
[3] V.J. Inglezakis, M.A. Stylianou, D. Gkantzou, M.D. Loizidou, Removal of Pb(II) from aqueous solutions by using clinoptilolite and bentonite as adsorbents, Desalination 210 (2007) 248–256.
[4] I. Chaari, E. Fakhfakh, S. Chakroun, J. Bouzid, N. Boujelben, M. Feki, F. Rocha, F. Jamoussi, Lead removal from aqueous solutions by a Tunisian smectitic clay, J. Hazard. Mater. 156 (2008) 545–551.
[5] F. Luo, Y. Liu, X. Li, Z. Xuan, J. Ma, Biosorption of lead ion by chemically-modified biomass of marine brown algae *Laminaria japonica*, Chemosphere 64 (2006) 1122–1127.
[6] A. Sarı, M. Tuzen, Biosorption of Pb(II) and Cd(II) from aqueous solution using green alga (*Ulva lactuca*) biomass, J. Hazard. Mater. 152 (2008) 302–308.

[7] T. Halttunen, S. Salminen, R. Tahvonen, Rapid removal of lead and cadmium from water by specific lactic acid bacteria, Int. J. Food Microbiol. 114 (2007) 30–35.

[8] C. Saka, Ö. Şahin, M.M. Küçük, Applications on agricultural and forest waste adsorbents for the removal of lead(II) from contaminated waters, Int. J. Environ. Sci. Technol. 9 (2012) 379–394.

[9] S. Sen Gupta, K.G. Bhattacharyya, Kinetics of adsorption of metal ions on inorganic materials: A review, Adv. Colloid Interface Sci. 162 (2011) 39–58.

[10] A. Ngomsik, A. Bee, M. Draye, G. Cote, V. Cabuil, Magnetic nano- and microparticles for metal removal and environmental applications: A review, C.R. Chimie 8 (2005) 963–970.

[11] N.N. Nassar, Rapid removal and recovery of Pb(II) from wastewater by magnetic nanoadsorbents, J. Hazard. Mater. 184 (2010) 538–546.

[12] Y. Tang, S. Liang, J. Wang, S. Yu, Y. Wang, Amino-functionalized core–shell magnetic mesoporous composite microspheres for Pb(II) and Cd(II) removal, J. Environ. Sci. 25(4) (2013) 830–837.

[13] A.S. de Dios, M.E. Díaz-García, Multifunctional nanoparticles: Analytical prospects, Anal. Chim. Acta 666 (2010) 1–22.

[14] M. Mahdavi, M.B. Ahmad, M.J. Haron, Y. Gharayebi, K. Shameli, B. Nadi, Fabrication and characterization of SiO_2/(3-aminopropyl)triethoxysilane-coated magnetite nanoparticles for lead(II) removal from aqueous solution, J. Inorg. Organomet. Polym. 23 (2013) 599–607.

[15] X. Xin, Q. Wei, J. Yang, L. Yan, R. Feng, G. Chen, B. Du, H. Li, Highly efficient removal of heavy metal ions by amine-functionalized mesoporous Fe_3O_4 nanoparticles, Chem. Eng. J. 184 (2012) 132–140.

[16] J. Wang, S. Zheng, Y. Shao, J. Liu, Z. Xu, D. Zhu, Amino-functionalized Fe_3O_4@SiO_2 core–shell magnetic nanomaterial as a novel adsorbent for aqueous heavy metals removal, J. Colloid Interface Sci. 349 (2010) 293–299.

[17] I.F. Nata, G.W. Salim, C. Lee, Facile preparation of magnetic carbonaceous nanoparticles for Pb^{2+} ions removal, J. Hazard. Mater. 183 (2010) 853–858.

[18] Y. Tan, M. Chen, Y. Hao, High efficient removal of Pb (II) by amino-functionalized Fe_3O_4 magnetic nanoparticles, Chem. Eng. J. 191 (2012) 104–111.

[19] S. Tao, C. Wang, W. Ma, S. Wu, C. Meng, Designed multifunctionalized magnetic mesoporous microsphere for sequential sorption of organic and inorganic pollutants, Microporous Mesoporous Mater 147 (2012) 295–301.

[20] G. Li, Z. Zhao, J. Liu, G. Jiang, Effective heavy metal removal from aqueous systems by thiol functionalized magnetic mesoporous silica, J. Hazard. Mater. 192 (2011) 277–283.

[21] Y. Zhu, J. Hu, J. Wang, Competitive adsorption of Pb (II), Cu(II) and Zn(II) onto xanthate-modified magnetic chitosan, J. Hazard. Mater. 221–222 (2012) 155–161.

[22] S. Singh, K.C. Barick1, D. Bahadur, Surface engineered magnetic nanoparticles for removal of toxic metal ions and bacterial pathogens, J. Hazard. Mater. 192 (2011) 1539–1547.

[23] A.Z.M. Badruddoza, Z.B.Z. Shawon, T.W.J. Daniel, K. Hidajat, M.S. Uddin, Fe_3O_4/cyclodextrin polymer nanocomposites for selective heavy metals removal from industrial wastewater, Carbohydr. Polym. 91 (2013) 322–332.

[24] H. Zhu, S. Jia, T. Wan, Y. Jia, H. Yang, J. Li, L. Yan, C. Zhong, Biosynthesis of spherical Fe_3O_4/bacterial cellulose nanocomposites as adsorbents for heavy metal ions, Carbohydr. Polym. 86 (2011) 1558–1564.

[25] S.S. Banerjee, D.H. Chen, Fast removal of copper ions by gum arabic modified magnetic nano-adsorbent, J. Hazard. Mater. 147 (2007) 792–799.

[26] Y.C. Chang, D.H. Chen, Preparation and adsorption properties of monodisperse chitosan-bound Fe_3O_4 magnetic nanoparticles for removal of Cu(II) ions, J. Colloid Interface Sci. 283 (2005) 446–451.

[27] A. Bée, D. Talbot, S. Abramson, V. Dupuis, Magnetic alginate beads for Pb(II) ions removal from wastewater, J. Colloid Interface Sci. 362 (2011) 486–492.

[28] A.F. Ngomsik, A. Bee, J.M. Siaugue, V. Cabuil, G. Cote, Nickel adsorption by magnetic alginate microcapsules containing an extractant, Water Res. 40 (2006) 1848–1856.

[29] A.F. Ngomsik, A. Bee, J.M. Siaugue, D. Talbot, V. Cabuil, G. Cote, Co(II) removal by magnetic alginate beads containing Cyanex 272®, J. Hazard. Mater. 166 (2009) 1043–1049.

[30] F. Ge, M.M. Li, H. Ye, B.X. Zhao, Effective removal of heavy metal ions Cd^{2+}, Zn^{2+}, Pb^{2+}, Cu^{2+} from aqueous solution by polymer-modified magnetic nanoparticles, J. Hazard. Mater. 211–212 (2012) 366–372.

[31] N.V. Jarvis, J.M. Wagener, Mechanistic studies of metal ion binding to water-soluble polymers using potentiometry, Talanta 42(2) (1995) 219–226.

[32] H.M. Jiang, Z.P. Yan, Y. Zhao, X. Hu, H.Z. Lian, Zincon-immobilized silica-coated magnetic Fe_3O_4 nanoparticles for solid-phase extraction and determination of trace lead in natural and drinking waters by graphite furnace atomic absorption spectrometry, Talanta 94 (2012) 251–256.

[33] M. Amara, H. Kerdjoudj, Modification of the cation exchange resin properties by impregnation in polyethyleneimine solutions—Application to the separation of metallic ions, Talanta 60 (2003) 991–1001.

[34] B. Gao, F. An, K. Liu, Studies on chelating adsorption properties of novel composite material polyethyleneimine/silica gel for heavy-metal ions, Appl. Surf. Sci. 253 (2006) 1946–1952.

[35] L. Lebrun, F. Vallée, B. Alexandre, Q.T. Nguyen, Preparation of chelating membranes to remove metal cations from aqueous solutions, Desalination 207 (2007) 9–23.

[36] I.W. Mwangi, J.C. Ngila, Removal of heavy metals from contaminated water using ethylenediamine-modified green seaweed (*Caulerpa serrulata*), Phys. Chem. Earth 50–52 (2012) 111–120.